Scientific Reports

https://doi.org/10.1038/s41598-026-51670-0

Article in Press

A validated method for contact angle measurement of low surface tension fluids using a modified Wilhelmy plate technique

Received: 18 December 2025

Accepted: 29 April 2026

Published online: 07 May 2026

Cite this article as: Fusina L., Tancon M., Casarin F. *et al.* A validated method for contact angle measurement of low surface tension fluids using a modified Wilhelmy plate technique. *Sci Rep* (2026). https://doi.org/10.1038/s41598-026-51670-0

Luca Fusina, Marco Tancon, Fabio Casarin, Maria Basso, Elena Colusso, Stefano Bortolin & Marco Azzolin

A validated method for contact angle measurement of low surface tension fluids using a modified Wilhelmy Plate Technique

Luca Fusina, Marco Tancon*, Fabio Casarin, Maria Basso, Elena Colusso,

Stefano Bortolin, Marco Azzolin

Department of Industrial Engineering, University of Padova,
Via Venezia 1, 35131 Padova, Italy

*Corresponding author:

Dr. Marco Tancon
Department of Industrial Engineering, University of Padova
Via Venezia 1, 35131 Padova, Italy
E-mail: marco.tancon@unipd.it

Abstract

The wettability of a liquid on a solid surface is a critical parameter in numerous fields, from microfluidics to heat transfer applications. At the microscale, it directly governs droplet mobility on engineered surfaces, with implications for phase-change heat transfer, fluid transport, and interfacial phenomena. However, the characterization of wettability, commonly quantified through contact angle measurements, is particularly challenging for many fluids employed in thermal devices. These fluids usually have low surface tension values resulting in small contact angles, and their normal boiling point below ambient temperature precludes measuring contact angles in open environments. Here, we present a modified optical Wilhelmy method to address these problems by measuring contact angles inside a pressure vessel under saturated conditions. Particular attention was dedicated to validate the technique against the standard sessile drop method at atmospheric conditions and to provide a rigorous uncertainty estimation. Results obtained with two low Global Warming Potential refrigerants, R1234ze(E) and R1233zd(E), demonstrate that the developed technique enables accurate and reproducible contact angle measurements, even below 10°. The technique provides a robust and practical tool for screening surface treatments and identifying those most effective for specific applications, including the promotion of dropwise condensation with refrigerants.

Keywords

Contact angle measurements, Optical Wilhelmy plate method, Surface wettability, Low surface tension fluids, Droplet mobility

Introduction

Understanding and accurately characterizing the wettability of a liquid on a solid surface is crucial in numerous fields, including microfluidics, interfacial transport, film stability in coating processes, water harvesting, and anti-icing [1–4], and becomes even more critical in high-pressure applications, such as spray cooling, boiling heat transfer, and CO_2 geo-sequestration [5]. Wettability determines droplet mobility on surfaces, which is essential for interfacial and phase-change processes. For example, dropwise condensation (DWC), which can significantly enhance heat transfer compared with filmwise condensation [6,7], occurs only when surface and fluid properties enable sufficient droplet mobility [8].

Despite this broad relevance, the reliable measurement of wettability, especially for low surface tension fluids and fluids with a normal boiling point (NBP) below ambient temperature, remains a significant experimental challenge. In this context, the present study introduces a new measurement methodology based on a modified optical Wilhelmy technique, to quantify both static and dynamic contact angles of low-surface-tension fluids under saturated conditions.

Wettability is typically characterized by means of contact angle measurements [9,10]. The equilibrium contact angle θ_e can be described as the angle formed when a liquid droplet is deposited onto an ideal surface, governed by Young's equation [11–13]. However, on real experimental specimens, inevitable surface heterogeneities cause deviations from this ideal behavior. In practice, it is only possible to approach this theoretical value. In general, on real surfaces, a static contact angle θ_s can be observed, between the two limit values called advancing θ_a and receding θ_r angles [12,14]. θ_a is the angle beyond which a droplet's contact line starts to move forward, towards a non-wetted surface. Conversely, the limit value below which the contact line starts to move through a wetted region is θ_r. Contact angle hysteresis is defined as the difference $\Delta\theta = \theta_a - \theta_r$ [15]. Surfaces exhibiting low hysteresis are generally associated with high droplet mobility, a desirable feature in many applications where control of liquid motion and adhesion are required [8].

Contact angles can be determined using optical techniques, such as the sessile drop, the capillary rise and the tilting-plate, or with force-based methods like the Wilhelmy plate technique [16]. With low surface tension fluids, the resulting contact angles are expected to be relatively low, often below 10°, highlighting the need for accurate measuring techniques. This

challenge is further amplified when dealing with many refrigerants used in heat transfer equipment because they have NBP below ambient temperature. As a consequence, under atmospheric conditions these fluids cannot remain liquid, preventing the use of standard contact-angle measurement techniques, such as the sessile-drop method [17]. However, they are of primary interest because many applications rely on the condensation of low-surface tension fluids, including refrigeration, air-conditioning, biofuels, chemical processes, data center cooling, Organic Rankine Cycles for power generation [18].

While the wettability of water and its role in DWC have been extensively studied [19], research on refrigerants remains limited. Previous studies have achieved DWC of ethanol and some hydrocarbons such as toluene, pentane and hexane, mainly using lubricant-infused surfaces [18,20–22] or grafted polymer coatings fabricated by initiated chemical vapor deposition [23]. With focus on fluorinated refrigerants, wetting and DWC remain relatively unexplored. Some authors employed R141b, which, however, has a normal boiling point (NBP) of 32 °C (from REFPROP 10.0 [24]), enabling the use of the sessile drop or the capillary rise methods, under atmospheric conditions [25,26]. R141b has also liquid-vapor surface tension $\sigma = 0.019$ N m^{-1} at 20 °C, higher than several refrigerants reported hereafter.

Vadgama and Harris [27] measured quasi-static advancing contact angles of R134a on aluminium and copper plates inside a pressure vessel, by recording the meniscus on the plate. However, their setup did not allow receding contact angle measurements, which are crucial given the importance of $\Delta\theta$ for DWC promotion. They reported average advancing angles between 5.6° and 8.3° for aluminium, and between 5.1° and 6.5° for copper. Lu et al. [17] investigated static contact angles of R134a, R22, R290, R600a, R32 on cylindrical samples of copper, stainless steel and aluminium (2 mm diameter), partially immersed in a liquid pool under saturated conditions, finding values below 4° in all cases. Similar results were obtained by Xu et al. [28] for R134a and R1234ze(E).

More recently, Fazle Rabbi et al. [29] measured θ_a and θ_r for two low-surface tension refrigerants, R1233zd(E) and R1336mzz(Z), depositing a droplet on the test surface and then letting it evaporate inside a vessel. Using an omniphobic coating, they achieved $\theta_a = 26°$ with $\Delta\theta$ of 7° for R1233zd(E), and $\theta_a = 28°$ with $\Delta\theta$ of 9° for R1336mzz(Z). This study demonstrated, for the first time, the feasibility of DWC of low-surface tension fluorinated refrigerants.

From the literature, there is little information on accurate and repeatable techniques to measure both advancing and receding angles of fluids with NBP below ambient temperature, while avoiding the complexities associated with controlling droplet deposition and evaporation. Furthermore, proper assessment of measurement uncertainty is usually lacking. Typically, only the standard deviation is reported, reflecting surface non-uniformity; however, this neglects significant contributions from the optical system and image analysis, which can substantially affect the overall uncertainty and should therefore be carefully assessed [30,31].

In the present study, we developed a measurement method based on a modified optical Wilhelmy technique, specifically designed to enable static and dynamic contact angle measurements of low-surface tension fluids on cylindrical samples under saturated conditions. Key aspects of the technique, including precise meniscus interpolation and the use of Monte Carlo simulations to quantify measurement uncertainty from image analysis, are discussed. The developed experimental technique was validated against the sessile drop method at ambient conditions, using different combinations of fluids (water, ethylene glycol, and ethanol) and surfaces (aluminium, copper, and PTFE), spanning a wide range of surface tensions and surface energies.

After validation, the technique was applied to two refrigerants under saturated conditions at pressures above ambient: the hydrofluoroolefin (HFO) R1234ze(E) and the hydrochlorofluoroolefin (HCFO) R1233zd(E). These two fluids were selected to demonstrate the capability of the present technique to measure contact angles of low-surface tension fluids under pressurized conditions. They were also chosen for their potential as medium-term replacements of hydrofluorocarbons (HFCs), due to their low flammability and low Global Warming Potential (GWP) [32,33]. The tested surfaces ranged from metals to PTFE and sol-gel silica-based coatings, which were already demonstrated to promote and sustain DWC of steam [34].

The primary contribution of this study is the development of a reliable procedure for quantifying contact angles of low surface tension fluids. This tool is critical for screening surfaces that optimize droplet mobility and wetting behavior in phase-change heat transfer, such as in DWC of refrigerants, and for providing accurate data needed to develop and validate predictive heat transfer models. As an additional outcome, the measurements reported here generate a valuable dataset addressing the current lack of contact angle data for refrigerants, supporting

further experimental and numerical studies. Finally, the technique can be applied in several contexts where contact angles must be measured under pressures above atmospheric.

Experimental methods

Sample preparation

Two kinds of samples were employed: flat (20 × 20 mm^2) for validation with the sessile drop method, and cylindrical (100 mm in length and 8 mm in diameter) for the newly developed optical Wilhelmy method. The same surface finish was obtained for both flat and cylindrical specimens, as described hereafter.

Three substrates were used, namely PTFE, aluminium, and copper. Copper and aluminium samples were treated with emery papers, progressively from #500 to #4000. The same surface finish was obtained for PTFE surfaces.

Furthermore, two hybrid organic-inorganic silica sol-gel coatings were prepared on aluminium substrates with the surface finish described above, hereafter named M7T3 and O2T8, following the protocols detailed in Parin et al. [35] and Basso et al. [34], respectively. The M7T3 sample was used in the validation phase, while the O2T8 one, more hydrophobic, was tested with the refrigerants. The employed reagents are: methyl-triethoxy-silane (MTES, 99%, Sigma-Aldrich), tetraethyl orthosilicate (TEOS, 98%, Sigma-Aldrich), octyltriethoxysilane (OTES, 98%; Sigma-Aldrich), used as purchased, as well as hydrochloric acid (1 M concentration, Merck), ethanol (EtOH, Merck) and ultrapure water (Chemlab). Sol-gel silica coating solutions were synthetized in an ethanolic solvent under acidic conditions. The sol-gel coatings were deposited on aluminium substrates by dip coating at a withdrawal speed of 10 cm min^{-1}. Finally, the coated samples were treated in furnace at 200 °C for 1 hour. As for the nomenclature, M, T and O stand for the reagents MTES, TEOS and OTES, respectively, while the numbers refer to the molar ratio of the reagents in the solution.

Surface roughness was determined with a KLA-Tencor P-17 stylus profiler. Morphological maps were acquired on a 200 µm × 200 µm area and analysed with the Apex Analysis Software. The surface energy γ of aluminium, PTFE, and coated samples was determined according to the OWRK method.

Experimental setup for the optical modified Wilhelmy method

Many common low surface tension fluids, as refrigerants, have normal boiling points below the ambient temperature, which makes it impractical to evaluate the wettability between the surface and the liquid refrigerant under atmospheric pressure. Therefore, a dedicated setup was developed inside a pressurized chamber to enable accurate dynamic contact angle measurements. Unlike the traditional Wilhelmy plate method, in which a sample is fixed to a force sensor and immersed into or withdrawn from a liquid by vertically displacing the liquid container (i.e., a beaker), with contact angles determined from the corresponding force measurements [36], the present study employed a modified Wilhelmy plate technique.

In this configuration, the same principle of controlled sample movement is maintained; however, the contact angles are obtained through optical measurements, which offers greater simplicity and robustness when operating in a pressurized chamber. Fig.1 shows the experimental apparatus and refrigerant circuit, with an overview of the pressurized chamber in Fig.1a, including the refrigerant lines and the positioning of the LED light and camera at two diametrically opposite locations. Fig. 1b depicts the interior of the chamber, including the refrigerant line with the capillary tube and the beaker mounted on a motorized translation stage. The setup also includes a refrigerant filling line from a tank and a vent line to a secondary tank for refrigerant recovery after testing.

Before filling the chamber with the test fluid, the sample is mounted at the top of the chamber, and the system is evacuated using a vacuum pump (valve V2 open, valve V1 closed). The chamber is then filled with the fluid. When a refrigerant is used, vapor is first introduced through a capillary tube while the pressure is increased to the saturation pressure at ambient temperature. Subsequently, liquid refrigerant is added through the same capillary to fill the beaker. Saturated conditions were verified by monitoring the chamber temperature with a Pt100 (1/3 DIN accuracy class) and the pressure with a calibrated transducer (Endress+Hauser Cerabar S, accuracy ±0.05 bar), ensuring the absence of non-condensable gases and the stability of the system throughout the measurements.

After the filling stage, the measurement can take place: the beaker, containing the liquid refrigerant and mounted on a motorized translation stage (Thorlabs® MTS25/M-Z8 – 25 mm, declared accuracy: 60 µm), moves vertically and as it is lifted, the sample (Fig. 1c) is gradually immersed, allowing the advancing contact angle to be captured. After pausing the stage, the

static contact angle is measured before the beaker is lowered, during which the receding contact angle is recorded. The motorized movements allow high measurement reproducibility, and enable accurate control of the contact line movement. This capability is particularly advantageous when measuring very low receding contact angles, for which droplets in sessile drop experiments may exhibit contact line pinning.

During the experiment, the beaker translation velocity was set at 0.05 mm s^{-1}, based on the results discussed later in the manuscript (see Section “Dynamic contact angles” in the “Results and Discussion”). The actual translation velocity was verified through image analysis of the camera recordings, showing a deviation of less than 4% from the setpoint. For each test, the sample is first immersed inside the liquid pool for at least 5 mm, to minimize edge effects. It is then further immersed at constant velocity over a length of at least of 5 mm within the “measuring section” indicated in Fig. 1c, during which the advancing contact angles are recorded. After the motor is stopped, the static contact angle is measured. Subsequently the sample is withdrawn at constant velocity over a distance of at least 5 mm to record the receding contact angles. For static contact angles, the procedure is repeated at multiple positions along the length of the cylinder.

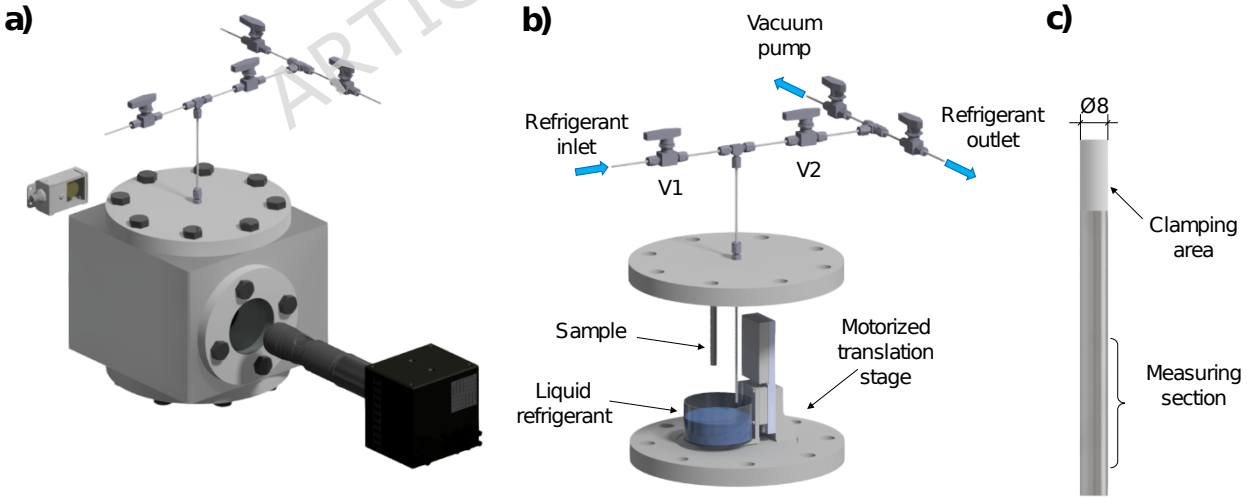

Fig. 1. Experimental apparatus for contact angle measurements using the modified Wilhelmy method. a) Pressurized chamber and optical system with LED source and high-speed camera; b) setup inside the chamber; c) 8 mm diameter cylindrical sample.

Images were taken through one viewport by a high-speed camera (Photron® FASTCAM Mini UX100, Tokyo, Japan) equipped with a microscopic lens (Navitar® ZOOM 12X, Rochester, NY, USA), providing a resolution of 1280 × 1024 pixels and 10 µm per pixel. A 3× zoom was employed in the following analyses. Uniform illumination from an LED source at the opposite viewport, combined with a diffusing sheet, ensured clear visualization of the liquid-vapor interface.

The cylindrical samples (Fig. 1c) provide a clearer view of the meniscus, with respect to the flat plates commonly employed in the Wilhelmy method [17]. To avoid distortions of the meniscus shape, the cylinder radius was always chosen to be larger than the capillary length $\lambda_c = \sqrt{\sigma/\rho g}$ of the fluids, as reported in Table 1 [15].

The present method is applicable only to contact angles below 90°, as the meniscus is not clearly visible at higher angles. In fact, when angles are above 90° the meniscus is oriented downwards, and cannot be accurately resolved with a horizontal camera since the liquid pool in the beaker covers the interface. Nevertheless, this limitation does not pose a significant issue, given the small contact angles expected for low-surface tension refrigerants [17,29].

Data reduction and uncertainty analysis

The image processing and analysis procedure, carried out in MATLAB®, is illustrated in Fig. 2. Images captured with the high-speed camera were first converted to grayscale. The vertical wall of the cylindrical sample as well as the interface between liquid and vapor phases were then identified by means of a custom code based on the algorithm developed by Trujillo-Pino et al. [37]. Next, the liquid-vapor interface was fitted using polynomial interpolation, while the wall profile was interpolated by a straight line. The contact point between the meniscus and the vertical wall was identified from the intersection of the two fits, and the contact angle was then calculated from the tangent to the meniscus evaluated at this point.

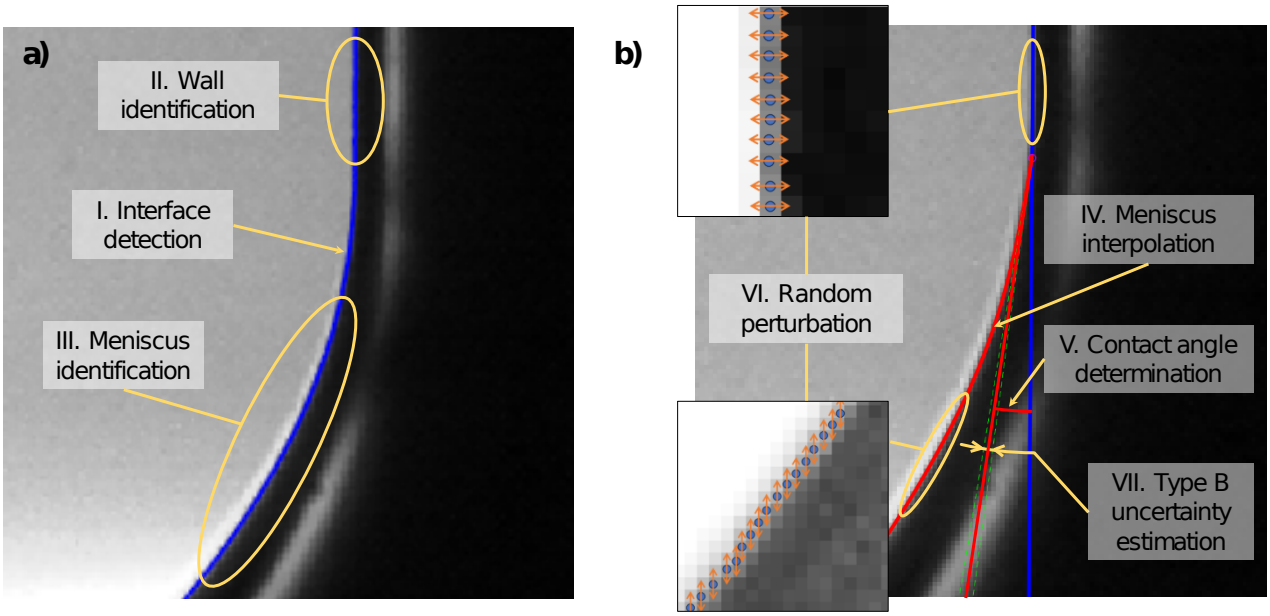

Fig. 2. Procedure for contact angle determination from image analysis. a) Selection of vertical wall and liquid-vapor interface portion. b) Calculation of the contact angle and uncertainty estimation from Monte Carlo simulations.

The degree of the polynomial used to interpolate the meniscus profile, as well as the number of points selected along the profile, may affect the measurements. Therefore, several images with angles between 0° and 90° were analyzed to obtain optimal sets of interpolation parameters for each angle range. Throughout the study, the polynomial degree was selected within the identified range following a convergence criterion, i.e., by choosing the lowest degree at which the fitting error reaches a plateau and provides a stable extrapolation of the interface near the wall (see Supplementary Section S1).

When contact angles are evaluated at different positions on a surface, the standard deviation is usually reported as an indicator of surface uniformity. Nevertheless, the standard deviation is not sufficient to describe the variability of the measurements, since contact angle measurements by optical methods suffer from errors that cannot be neglected, particularly at very small or very large angles (approaching 180°) where the interpolation of the interface might give higher uncertainty. Such errors in contact angle measurement, in particular with sessile drops, are commonly reported to be at least 2° [38], but can increase up to ±8° for angles above 150° [39]. With the aim of providing a reliable indicator of the average characteristics of a surface, the following procedure is proposed, based on the JCGM guidelines

[40]. For each measurement, two values are reported: the mean value, averaged over different positions on the sample surface, and an expanded uncertainty including the Type A, $u_A(\theta)$, and the Type B, $u_B(\theta)$, contributions.

The Type A standard uncertainty, Eq. 1, is determined from repeated measurements performed at different positions along the sample surface, providing an estimate of the surface uniformity:

$$u_A(\theta) = \frac{\sigma_N}{\sqrt{N}} \tag{1}$$

where σ_N is the standard deviation of the N measurements carried out at different positions.

The combined uncertainty $u_C(\theta)$ is then calculated (Eq. 2), including the Type B uncertainty contribution coming from image processing and contact angle determination via software:

$$u_C(\theta) = \sqrt{u_A^2(\theta) + u_B^2(\theta)} \tag{2}$$

Regarding the Type B uncertainty, Monte Carlo simulations have been performed to estimate the influence of variations in the points defining the liquid-vapor interface on the contact angle measured by the present technique. This approach accounts for possible distortions and noise arising from external causes, such as light reflections inside the chamber, and provides an estimate of the measurement uncertainty, according to the procedure described in Guimarães Couto et al. [41].

In particular, after obtaining the coordinates of the points along the meniscus and the vertical wall, the vertical positions of the liquid-vapor interface points and the horizontal positions of the wall points are randomly perturbed (Fig. 2b). The artificial noise has a normal distribution with a standard deviation of 1 pixel, accounting for the optical setup and the sub-pixel edge detection tool. After the perturbation, the interpolation and the contact angle measurement are carried out. The procedure is then repeated for 2×10^5 simulations, randomly varying the perturbations. Finally, the standard deviation of the contact angle is taken as Type B uncertainty.

The value of u_B was investigated for different angles, between 0° and 90°, in particular to see if there is a trend against the angle to be measured. Different simulations were carried out (see

Supplementary Section S1.4), and it was observed that the disturbances affect the results similarly in any conditions, regardless of the magnitude of the contact angle under investigation, when calculating the contact angle with the procedure described above and accounting for the issues detailed in Supplementary Sections S1.2 and S1.3. Hence, an average value $u_B = 0.5°$ was estimated and assumed in the following analysis.

Due to the limited number of measurements typically carried out for contact angles (in general, $N < 10$), the coverage factor k_p for the expanded uncertainty is obtained from Student's t-distribution. The confidence level is set equal to $p = 95\%$. As for the effective degrees of freedom ν_{eff}, the Welch-Satterthwaite formula has been employed, considering $\nu_A = N$-1 degrees of freedom for the Type A term and $\nu_B \to \infty$ for the Type B term:

$$\nu_{\mathrm{eff}} = \frac{u_C^4(\theta)}{\frac{u_A^4(\theta)}{\nu_A}} \tag{3}$$

The expanded uncertainty is finally:

$$U(\theta) = k_p u_C(\theta) \tag{4}$$

with a coverage factor k_p generally between 2 and 3. Accordingly, each reported angle in this study is the average of at least five independent measurements at different locations on the surface, with the corresponding expanded uncertainty.

In the present study, the uncertainty in contact angle measurements is typically within 1 – 2°. As the contact angle approaches 0°, however, the relative uncertainty increases significantly: for contact angles around 3 – 4°, it can reach ~50% of the measured value. Therefore, this 3 – 4° range should be considered a practical lower limit of the technique. Albeit not being a strict threshold, it should be taken as a reference, below which measurements can only be taken as indicative of nearly complete wetting, in agreement with the literature [17]. This physical limit is also driven by optical resolution constraints and image noise, which make it increasingly difficult to distinguish the liquid-vapor interface from the vertical wall at such low angles.

Results and Discussion

A comprehensive validation of the newly developed technique, based on the modified Wilhelmy method, is presented through direct benchmarking against the conventional sessile drop technique. The study first consolidates the accuracy of static contact angle measurements and then, upon identifying the optimal velocity for precise wettability evaluation, characterizes dynamic contact angle behavior. For the sessile drop procedure, droplets of volume ~10 µL were deposited at an average rate of ~1 µL s^{-1} [6,42] (see Supporting Section S1). Finally, the applicability of the method under non-ambient pressure conditions is demonstrated for the two low-GWP refrigerants R1234ze(E) and R1233zd(E).

Three reference fluids were employed for validation purposes: water, ethylene glycol, and ethanol. Their thermophysical properties are reported in Table 1. These three fluids were selected for their progressively lower surface tension, and since they can be tested under atmospheric conditions, as all three possess normal boiling points above ambient temperature. In contrast, the refrigerants R1234ze(E) and R1233zd(E) have NBPs below 20 °C; their thermodynamic and transport properties are reported in Table 1. With regards to the surfaces, flat samples were prepared for sessile drop measurements following the same procedures used for the cylindrical samples.

For the validation campaign, aluminium, copper, polytetrafluoroethylene (PTFE) were tested, together with the hybrid sol-gel methyl-silica (M7T3) and hybrid sol-gel octyl-silica (O2T8) coatings. Measurements with the two refrigerants were performed on aluminium, PTFE, and O2T8 surfaces. M7T3 was chosen as a representative smooth coating with moderate hydrophobicity, providing uniform surface properties suitable for contact angle measurements. Moreover, M7T3 exhibits contact angles below 90° for all the three fluids considered for validation, allowing the application of the modified Wilhelmy method. On the other hand, PTFE and O2T8 were identified as first possible candidates for studies with low-surface tension fluids, with O2T8 preferred over M7T3 due to its higher hydrophobicity [34].

Table 1. Liquid-vapor surface tension, normal boiling point NBP (at 1 atm), liquid density and capillary length of tested fluids, taken from REFPROP 10.0 [24]. Thermodynamic and transport properties are calculated at 20 °C.

Fluid	σ [mN m^{-1}]	NBP [°C]	ρ [kg m^{-3}]	λ_c [mm]
Water	72.7	100.0	998	2.73
Ethylene glycol	48.7	197.2	1113	2.11
Ethanol	22.4	78.4	789	1.70
R1234ze(E)	9.6	-19.0	1179	0.91
R1233zd(E)	15.2	18.3	1275	1.10

Static contact angles

As the first step of the validation procedure, the modified Wilhelmy method was compared against the standard sessile drop method for static contact angle measurements under atmospheric conditions. The three fluids (water, ethylene glycol, ethanol) were tested on both flat and cylindrical samples with identical surface finishes. Table 2 reports the static contact angles measured on aluminium, copper, PTFE, M7T3, and O2T8 samples. As previously discussed, the present method is not suitable for contact angles exceeding 90°, and therefore measurements for water on PTFE and O2T8 were omitted for the optical Wilhelmy method.

Table 2. Comparison of static contact angles measured by standard sessile drop and present (optical Wilhelmy) methods, with the experimental uncertainty calculated following the procedure described in Section “Data reduction and uncertainty analysis”. The values for water on PTFE and O2T8 are omitted because the angle is above 90°.

Surface	Method	Water	Ethylene glycol	Ethanol
Aluminium	Sessile drop	64.4° ± 3.7°	48.5° ± 5.8°	10.6° ± 5.9°
	Present method	68.3° ± 1.9°	49.1° ± 2.0°	10.3° ± 1.9°
Copper	Sessile drop	59.3° ± 3.3°	43.9° ± 1.0°	9.3° ± 3.3°
	Present method	59.6° ± 4.8°	43.6° ± 1.5°	7.8° ± 1.6°
PTFE	Sessile drop	104.4° ± 3.1°	82.5° ± 2.3°	48.0° ± 1.8°
	Present method	-	79.1° ± 1.6°	48.7° ± 3.3°
M7T3	Sessile drop	79.9° ± 3.5°	57.1° ± 3.0°	12.4° ± 3.0°
	Present method	80.2° ± 2.1°	56.6° ± 1.7°	10.0° ± 1.3°
O2T8	Sessile drop	93.0° ± 4.0°	72.0° ± 1.4°	18.2° ± 2.8°

Present method	-	73.1° ± 1.2°	20.1° ± 2.1°

The agreement between the two techniques was found to be within the measurement uncertainty for all fluid-surface combinations, with a maximum difference of 3.9° in the case of water on bare aluminium. Static contact angles on copper surfaces are shown in Fig. 3 for water, ethylene glycol and ethanol, to provide a visual comparison between the sessile drop method (Fig. 3 a, b, c) and the modified Wilhelmy method (Fig. 3 d, e, f). The influence of surface tension σ is evident, with progressively lower θ_s values as σ decreases moving from left to right in Fig. 3.

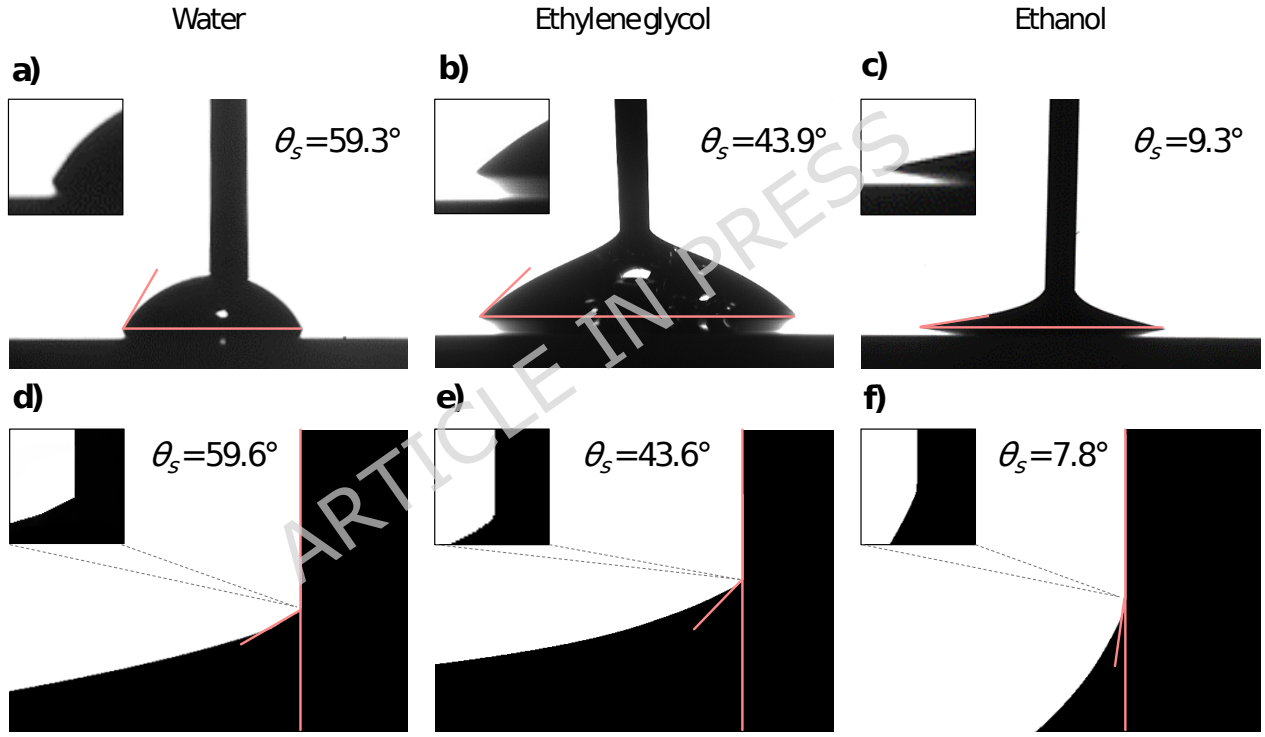

Fig. 3. Comparison of static contact angles (θ_s) measured on copper with the sessile drop method (top figures) and with the present technique (bottom), for water (a, d), ethylene glycol (b, e), and ethanol (c, f), respectively.

Dynamic contact angles

Static contact angles alone cannot fully describe the wetting behavior of a liquid on a solid surface. The mobility of the contact line plays a crucial role in interfacial dynamics, highlighting the relevance of contact angle hysteresis [8]. To perform dynamic contact angle measurements

with the modified Wilhelmy technique, a regime of forced spreading [43] must be established through a proper selection of the immersion and withdrawal velocities. Accordingly, the effect of velocity on the measured angles was first investigated, followed by a comparison with the sessile drop method to further validate the technique under dynamic conditions involving moving contact lines. These results are reported in Fig. 4. Error bars are included for all data points in Figs. 4a and 4c (in some cases smaller than the symbol size), whereas they are not shown in Fig. 4b, as each point corresponds to a single local measurement rather than to an average over repeated measurements.

The advancing and receding contact angles of water on the M7T3 coated sample were measured at 13 velocities between 0.01 mm s^{-1} and 0.2 mm s^{-1}, as shown in Fig. 4a. Based on these results, a velocity 0.05 mm s^{-1} was set for all the subsequent tests, since both θ_a and θ_r vary by less than 1.3° in the range from 0.01 □ 0.05 mm s^{-1}. This variation is considered acceptable in light of the measurement uncertainty and inherent surface non-uniformity, and this choice allows to minimize the time required for the tests without appreciably affecting the results.

The effect of velocity becomes more and more evident as velocity increases. Indeed, from the minimum to the maximum investigated velocity, θ_a increased by 4.4° (+5.4%) and θ_r decreased by 8.7° (-14.4%). These two opposite trends are confirmed by the literature [14,44,45], while the selected velocity falls within the recommended range for several measurement methods, including the Wilhelmy plate technique [36,46]. In this work, the term “dynamic contact angle” is used to distinguish advancing and receding angles from the static angle. Other authors refer to these angles as quasi-static, reserving the definition of dynamic angles only for cases where velocity significantly affects the measurements, as observed here. Hence, it is possible to define static θ_a and θ_r in addition to dynamic θ_a and θ_r [14,16]. Since it was found that the angles are not significantly affected by velocity below 0.05 mm s^{-1}, the term dynamic angles will be used throughout this work, while higher velocity values are not considered.

The present technique also enables measurements at different heights along the sample, allowing the assessment of potential variations in wetting behavior along its length as well as at different angular positions. Accordingly, both θ_a and θ_r were measured 10 times at steps of 0.25 mm along the longitudinal direction of the sample. These values were taken sufficiently far from the sample’s bottom edge to avoid any border effect. The results for ethylene glycol on the M7T3 sample (Fig. 4b) show a standard deviation of 1.2° and 0.7° for the advancing and

the receding angles, respectively. In the rest of the manuscript, a similar procedure is applied: local measurements at multiple locations are averaged, and the corresponding expanded uncertainty is reported.

For the validation of the present method in the case of dynamic contact angles, measurements were carried out with the M7T3 coated sample at ambient conditions of temperature and pressure, using the selected velocity of 0.05 mm s^{-1}. Results for θ_a and θ_r are presented in Fig. 4c, demonstrating compatibility between the two methods. The maximum difference of 3° was observed for θ_a in the case of ethanol, still within the experimental uncertainty. These results further demonstrate that the present method can reliably measure low contact angles, i.e., around 10° or lower, a feature that is crucial for characterizing the wettability of low-surface tension fluids.

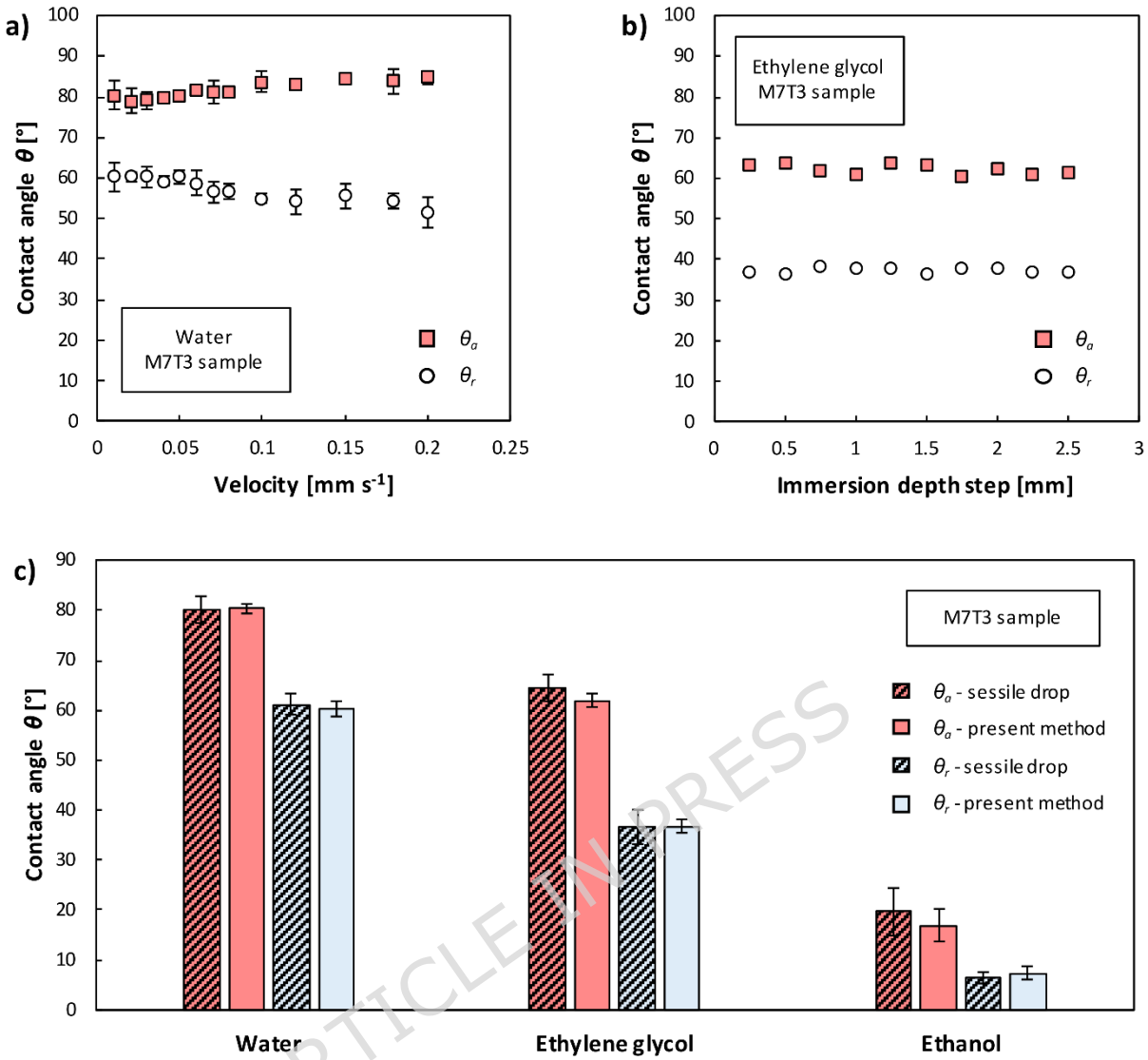

Fig. 4. Dynamic contact angle measurements on the M7T3 coated sample. a) Effect of immersion and withdrawal velocity on advancing (θ_a) and receding (θ_r) contact angles with water. b) Measurements at different positions along the sample length for ethylene glycol. c) Summary of the validation results. Comparison of θ_a and θ_r calculated according to the sessile drop method (hatch-filled columns) and the present modified optical Wilhelmy technique (empty columns).

Contact angle measurements of refrigerants R1234ze(E) and R1233zd(E)

After validating the developed technique for both static and dynamic contact angle measurements, the wettability of two refrigerants with NBP below ambient temperature, R1234ze(E) and R1233zd(E), was experimentally investigated. Unlike the previous measurements, these tests require the use of the pressurized chamber described in Section

"Experimental methods". In fact, their saturation pressure at 20 °C is 4.27 bar and 1.08 bar, respectively. The low contact angles expected for these two low surface tension refrigerants impose further attention in meniscus interpolation and contact angle calculation. It should be noted that comprehensive wettability measurements with detailed uncertainty analysis involving low surface tension fluids are rare in the literature, especially for the two refrigerants examined in this study, despite their relevance in the current scenario of phasing down or out high-GWP refrigerants [47–50].

For R1234ze(E), a baseline aluminium sample was tested in comparison with PTFE and O2T8 samples. Under ambient conditions, PTFE typically exhibits advancing and receding contact angles of around 130° and 90° with water, respectively [51], whereas O2T8 is characterized by $\theta_a \approx 100°$ and $\theta_r \approx 90°$ [34]. Furthermore, alkyl-terminated flat sol-gel hybrid films (such as O2T8) have been reported to exhibit dynamic dewetting toward various liquids, a "liquid-like" behavior attributed to the high mobility of the surface-tethered alkyl chains [52–54].

Fig. 5 **s**hows the surface characteristics of the samples in terms of root mean square roughness (Sq) and surface energy (see the "Experimental methods" and section S4 in the Supporting Information for further details). Both aluminium and PTFE displays a similar Sq of about 80 nm, whereas the coated sample exhibit a lower roughness of approximately 50 nm. The surface energies estimated according to the OWRK method are 39.1 mJ m^{-2}, 16.6 mJ m^{-2} and 26.6 mJ m^{-2} for aluminium, PTFE and O2T8, respectively.

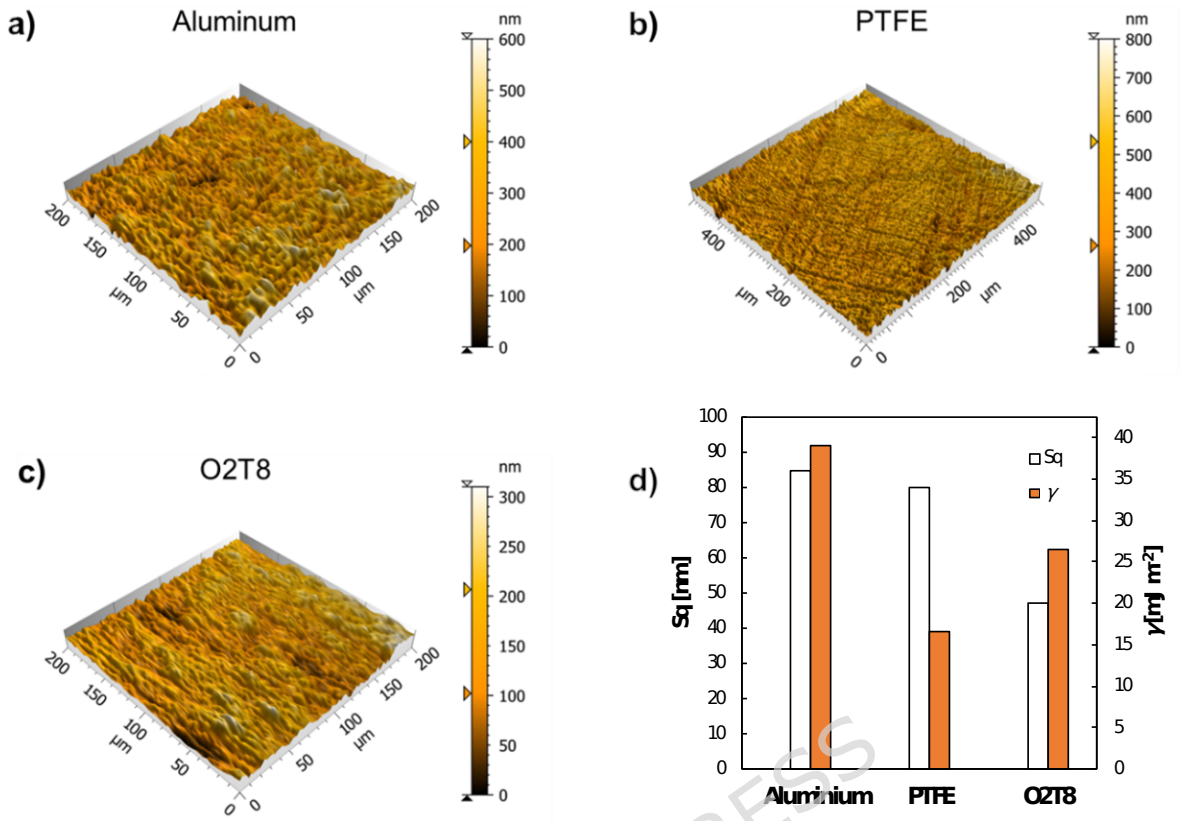

Fig. 5. Profilometer map of the sample surface of aluminium (a), PTFE (b) and O2T8 (c). d) Surface roughness (Sq) and surface energy (γ) values of the tested samples.

The contact angles obtained with the two refrigerants are shown in Fig. 6, while an example of contact angle visualizations for R1233zd(E) is provided in Fig. S4. On bare aluminium, R1234ze(E) displays θ_a = 5.6° and θ_r = 2.3°. Considering the measurement uncertainty and the receding contact angle approaching 0°, R1234ze(E) can be considered to completely wet the substrate. The static contact angle was found to be θ_s = 5.3°, in close agreement with the value of 6.4° reported by Xu et al. [28] for R1234ze(E) on copper with a similar surface finish, optically measured on a flat sample inside a vessel. These low values are consistent with the behavior expected for high surface energy materials such as metals [55,56], which typically exhibit nearly complete wetting.

Fig. 6a illustrates that contact angles increase when moving from aluminium to PTFE and O2T8, with θ_a exceeding 8°, and a non-zero receding angle. The difference between advancing and receding angles falls within the experimental uncertainty. For the other refrigerant, R1233zd(E), the advancing angle on O2T8 is about 1° higher than on PTFE, but the contact angles remain very similar to those for R1234ze(E).

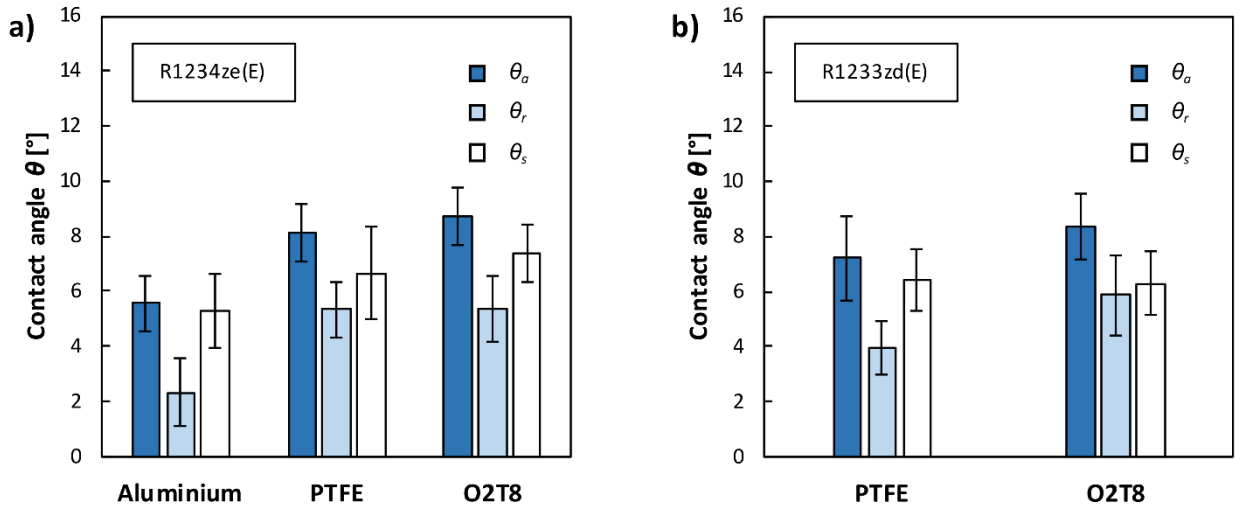

Fig. 6. Dynamic and static contact angles measured with the modified Wilhelmy method. a) Contact angles of R1234ze(E) on aluminium, PTFE and O2T8. b) Contact angles of R1233zd(E) on PTFE and O2T8.

In all cases, the angles are below 10°. Focusing first on the static contact angles, ideally equal to the equilibrium contact angle θ_e, some observations can be drawn from Young's equation [11], which relates the static contact angle to the interfacial free energies of the liquid-vapor (σ_{lv} or simply σ), solid-vapor (σ_{sv} or γ), and solid-liquid (σ_{sl}) interfaces:

$$\cos(\theta) = \frac{\sigma_{sv} - \sigma_{sl}}{\sigma_{lv}} \quad (5)$$

This relationship helps to rationalize the similarity in contact angles observed on the different surfaces. The liquid surface tension of the tested refrigerants (σ_{lv}) is extremely low (< 15 mN m^{-1}), falling below the surface energy of both PTFE (16.6 mJ m^{-2}) and O2T8 (26.6 mJ m^{-2}). Consequently, the system operates in a regime of near-complete wetting [57], with cos(θ) close to 1. However, deviations from Young's ideal conditions arise on real surfaces, where heterogeneities create energy barriers that arrest the contact line at finite angles [58,59]. To quantify this behavior, the spreading coefficient S was evaluated using the experimental contact angles via the relation $S = \sigma_{lv}(\cos\theta - 1)$. While $S > 0$ indicates complete wetting, values below zero correspond to partial wetting. For PTFE and O2T8, the calculated S values are comparable (about –0.08 mN m^{-1}) for both R1234ze(E) and R1233zd(E). This confirms that, despite their

different surface tensions, both fluids exhibit identical spreading tendency. In contrast, untreated aluminium results in S values even closer to zero (about –0.04 mN m^{-1}). This implies that the stronger spreading tendency on the untreated aluminium allows the fluid to further overcome surface heterogeneities, resulting in contact angles closer to the theoretical limit of zero.

It is worth noting that the measured static angle is generally closer to the advancing angle rather than the receding angle. This behavior is widely reported in the literature and is consistent with the physical nature of standard contact angle measurements (e.g., performed with the sessile drop method): both θ_a and θ_s evaluate the interaction of the liquid with an initially dry surface, whereas θ_r represents dewetting from a previously wetted area [60].

From an application perspective, the low contact angles measured for the two refrigerants may not be sufficient to sustain DWC. Cha et al. [8] proposed a map predicting the conditions under which DWC can be sustained, based on the Bond number, advancing contact angle and contact angle hysteresis. As θ_a decreases, $\Delta\theta$ must also decrease, and for advancing angles below 20°, the required contact angle hysteresis tends towards 0°. Moreover, highly wettable surfaces tend to promote higher nucleation density, which can increase the risk of flooding even at moderate saturation-to-wall temperature differences, potentially causing a transition to filmwise condensation [19]. Recently, Fazle Rabbi et al. [29] demonstrated that DWC of R1233zd(E) can be achieved on surfaces with surface energies of about 10 mJ/m^2, exhibiting θ_a of about 26°.

In this perspective, the present optical technique represents a valuable tool for investigating the wettability of low surface tension refrigerants with NBP below ambient temperature. Force-based measurements require either fragile sensors or balances, which can be impractical in small pressurized chambers, and careful data analysis to account for dynamic contributions, such as viscous forces [61,62]. In contrast, among currently available methods, the optical Wilhelmy offers a robust and simple alternative, also compared to approaches based on droplet deposition and evaporation. The technique enables accurate and reliable measurements of both static and dynamic contact angles even below 10°, and is sensitive to small variations in contact angle hysteresis, making it particularly suitable for the systematic screening of candidate surfaces for DWC applications, supporting the comparison among surfaces and helping identify directions for material design improvement.

Conclusions

Understanding and accurately characterizing surface wettability is essential in a wide range of applications, particularly when low surface tension fluids and pressurized conditions are involved. However, reliable contact angle data for fluids with normal boiling points below ambient temperature remain scarce, and measurements of advancing and receding contact angles are even more limited. In this work, a modified optical Wilhelmy technique was developed to enable static and dynamic contact angle measurements of low-surface tension fluids under saturated conditions inside a pressure vessel, together with a comprehensive assessment of measurement uncertainty.

The proposed method provides a robust and versatile tool for characterizing wettability and droplet mobility on cylindrical samples, overcoming limitations associated with droplet deposition, evaporation control, and optical resolution when dealing with very low contact angles. The technique was validated against the conventional sessile drop method at ambient conditions using several combinations of fluids (water, ethylene glycol, and ethanol) and solids: aluminium, copper, PTFE, and two hybrid sol-gel silica coatings (M7T3 and O2T8). The good agreement observed confirms the reliability of the approach and demonstrates its capability to resolve contact angles below 10° as well as subtle variations between different surfaces.

Following validation, the present method was applied to two low-surface tension refrigerants, R1234ze(E) and R1233zd(E), under saturated conditions. Measurements were performed on PTFE and O2T8 samples, providing new wettability data for fluid-surface pairs that were previously lacking in the literature. Both surfaces showed angles higher than the ones obtained on bare aluminium. In particular, O2T8 led to an increase in both advancing and receding contact angles of R1234ze(E), from 5.6° to 8.7° and from 2.3° to 5.4°, respectively, with a similar trend observed for PTFE. Regarding R1233zd(E), the contact angles on O2T8 were slightly higher than those on PTFE, most notably in terms of the receding angle, which increased from 4.0° to 5.9°.

Although the investigated surfaces do not appear suitable for sustaining dropwise condensation with the tested refrigerants, the results demonstrate the effectiveness of the developed technique in measuring very small contact angles under saturated conditions, making it a reliable screening tool for identifying surface treatments with improved wettability

characteristics for low-surface tension fluids with normal boiling points below ambient temperature.

Nomenclature

DWC = Dropwise Condensation

GWP = Global Warming Potential

HCFO = hydrochlorofluoroolefin

HFC = hydrofluorocarbon

HFO = hydrofluoroolefin

g = gravitational acceleration, m s^{-2}

k_p = coverage factor, -

N = number of experimental measurements

NBP = normal boiling point, °C

p = confidence level, -

S = spreading coefficient, mN m^{-1}

Sq = Root Mean Square Roughness, nm

u_A = Type A standard uncertainty

u_B = Type B standard uncertainty

u_C = combined standard uncertainty

U = expanded uncertainty

Greek symbols

γ = surface energy, mJ m^{-2}

$\Delta\theta$ = contact angle hysteresis, °

θ = contact angle, °

λ_c = capillary length, mm

ν = degrees of freedom

ρ = density, kg m^{-3}

σ = surface tension, mN m^{-1}

σ_N = standard deviation of N measurements

Subscripts

a = advancing

e = equilibrium

eff = effective

lv = liquid-vapor

r = receding

s = static

sl = solid-liquid

sv = solid-vapor

References

1. Gao, N. *et al.* How drops start sliding over solid surfaces. *Nat. Phys.* **14**, 191–196 (2018).
2. Mohammad Karim, A., Suszynski, W. J. & Pujari, S. Liquid film stability and contact line dynamics of emulsion liquid films in curtain coating process. *J. Coat. Technol. Res.* **18**, 1531–1541 (2021).
3. Abbatecola, A. *et al.* Understanding the Role of Superhydrophobicity on Heat Transfer Enhancement During Dropwise Condensation in Humid Air Flow. *Adv. Mater. Interfaces* **12**, 2500270 (2025).
4. Lv, J., Song, Y., Jiang, L. & Wang, J. Bio-inspired strategies for anti-icing. *ACS Nano* **8**, 3152–3169 (2014).
5. Song, J. W. & Fan, L. W. Understanding the effects of pressure on the contact angle of water on a silicon surface in nitrogen gas environment: Contrasts between low- and high-temperature regimes. *J. Colloid Interface Sci.* **607**, 1571–1579 (2022).
6. Li, S. *et al.* Durable, Ultrathin, and Antifouling Polymer Brush Coating for Efficient Condensation Heat Transfer. *ACS Appl. Mater. Interfaces* **16**, 1941–1949 (2024).
7. Abbatecola, A., Tancon, M., Fusina, L., Bortolin, S. & Del Col, D. Investigation of dropwise condensation of water at atmospheric and sub-atmospheric pressure through an individual-based model. *Appl. Therm. Eng.* **276**, 126892 (2025).
8. Cha, H. *et al.* Dropwise condensation on solid hydrophilic surfaces. *Sci. Adv.* **6**, eaax0746 (2020).
9. Marmur, A. Soft contact: measurement and interpretation of contact angles. *Soft Matter* **2**, 12–17 (2006).
10. Tancon, M. *et al.* Simultaneous measurement of heat flux and droplet population during dropwise condensation from humid air flowing on a vertical surface. *Exp. Therm. Fluid Sci.* **136**, 110677 (2022).
11. Young, T. An Essay on the Cohesion of Fluids. *Philos. Trans. R. Soc. Lond.* **95**, 65–87 (1805).
12. Ruiz-Cabello, F. J. M., Rodríguez-Valverde, M. A. & Cabrerizo-Vílchez, M. A. Equilibrium contact angle or the most-stable contact angle? *Adv. Colloid Interface Sci.* **206**, 320–327 (2014).

13. Villa, F., Marengo, M. & De Coninck, J. A new model to predict the influence of surface temperature on contact angle. *Sci. Rep.* **8**, 6549 (2018).

14. Butt, H. J. *et al.* Contact angle hysteresis. *Curr. Opin. Colloid Interface Sci.* **59**, 101574 (2022).

15. de Gennes, P. G., Brochard-Wyart, F. & Quéré, D. *Capillarity and Wetting Phenomena: Drops, Bubbles, Pearls, Waves*. (Springer, New York, 2004). doi:10.1007/978-0-387-21656-0.

16. Huhtamäki, T., Tian, X., Korhonen, J. T. & Ras, R. H. A. Surface-wetting characterization using contact-angle measurements. *Nat. Protoc.* **13**, 1521–1538 (2018).

17. Lu, X., Liu, J. & Xu, X. Contact angle measurements of pure refrigerants. *Int. J. Heat Mass Transf.* **102**, 877–883 (2016).

18. Sett, S. *et al.* Stable Dropwise Condensation of Ethanol and Hexane on Rationally Designed Ultrascalable Nanostructured Lubricant-Infused Surfaces. *Nano Lett.* **19**, 5287–5296 (2019).

19. Tancon, M. *et al.* Dropwise-to-filmwise transition during condensation of steam on hydrophilic surfaces. *Appl. Therm. Eng.* **278**, 127128 (2025).

20. Rykaczewski, K. *et al.* Dropwise condensation of low surface tension fluids on omniphobic surfaces. *Sci. Rep.* **4**, 4158 (2014).

21. Preston, D. J. *et al.* Heat Transfer Enhancement during Water and Hydrocarbon Condensation on Lubricant Infused Surfaces. *Sci. Rep.* **8**, 540 (2018).

22. Ho, J. Y., Rabbi, K. F., Sett, S., Wong, T. N. & Miljkovic, N. Dropwise condensation of low surface tension fluids on lubricant-infused surfaces: Droplet size distribution and heat transfer. *Int. J. Heat Mass Transf.* **172**, 121149 (2021).

23. Khalil, K. *et al.* Grafted Nanofilms Promote Dropwise Condensation of Low-Surface-Tension Fluids for High-Performance Heat Exchangers. *Joule* **3**, 1377–1388 (2019).

24. Lemmon, E. W., Bell, I. H., Huber, M. L. & McLinden, M. O. NIST Standard Reference Database 23: Reference Fluid Thermodynamic and Transport Properties-REFPROP, Version 10.0, National Institute of Standards and Technology. https://doi.org/10.18434/T4/1502528 (2018) doi:10.18434/T4/1502528.

25. Lin, L., Peng, H. & Ding, G. Influence of oil concentration on wetting behavior during evaporation of refrigerant-oil mixture on copper surface. *Int. J. Refrig.* **61**, 23–36 (2016).

26. Su, C. Y. *et al.* Pool Boiling Heat Transfer Enhanced by Fluorinated Graphene as Atomic Layered Modifiers. *ACS Appl. Mater. Interfaces* **12**, 10233–10239 (2020).
27. Vadgama, B. & Harris, D. K. Measurements of the contact angle between R134a and both aluminum and copper surfaces. *Exp. Therm. Fluid Sci.* **31**, 979–984 (2007).
28. Xu, W. *et al.* Experimental investigation on wettability of refrigerants on laser-ablated surfaces. *Colloids Surf. A Physicochem. Eng. Asp.* **665**, 131246 (2023).
29. Fazle Rabbi, K., Khodakarami, S., Ho, J. Y., Hoque, M. J. & Miljkovic, N. Dynamic omniphobic surfaces enable the stable dropwise condensation of completely wetting refrigerants. *Nat. Commun.* **16**, 1105 (2025).
30. Liu, K., Vuckovac, M., Latikka, M., Huhtamäki, T. & Ras, R. H. A. Improving surface-wetting characterization. *Science (1979).* **363**, 1147–1148 (2019).
31. Tripathy, A. *et al.* Ultrathin Lubricant-Infused Vertical Graphene Nanoscaffolds for High-Performance Dropwise Condensation. *ACS Nano* **15**, 14305–14315 (2021).
32. McLinden, M. O., Kazakov, A. F., Brown, J. S. & Domanski, P. A. A thermodynamic analysis of refrigerants: Possibilities and tradeoffs for Low-GWP refrigerants. *Int. J. Refrig.* **38**, 80–92 (2014).
33. Azzolin, M. *et al.* Local heat transfer measurements during in-tube condensation of refrigerants in a new test section made by additive manufacturing. *Appl. Therm. Eng.* **274**, 126689 (2025).
34. Basso, M. *et al.* Hydrophobic hybrid silica sol-gel coating on aluminium: Stability evaluation during saturated vapour condensation. *J. Non-Crystalline Solids: X* **17**, 100143 (2023).
35. Parin, R., Sturaro, M., Bortolin, S., Martucci, A. & Del Col, D. Heat transfer during dropwise condensation of steam over a mirror polished sol-gel coated aluminum substrate. *Int. J. Therm. Sci.* **144**, 93–106 (2019).
36. Wang, J. H., Claesson, P. M., Parker, J. L. & Yasuda, H. Dynamic Contact Angles and Contact Angle Hysteresis of Plasma Polymers. *Langmuir* **10**, 3887–3897 (1994).
37. Trujillo-Pino, A., Krissian, K., Alemán-Flores, M. & Santana-Cedrés, D. Accurate subpixel edge location based on partial area effect. *Image Vis. Comput.* **31**, 72–90 (2013).

38. Bateni, A., Susnar, S. S., Amirfazli, A. & Neumann, A. W. A high-accuracy polynomial fitting approach to determine contact angles. *Colloids Surf. A Physicochem. Eng. Asp.* **219**, 215–231 (2003).

39. Vuckovac, M., Latikka, M., Liu, K., Huhtamäki, T. & Ras, R. H. A. Uncertainties in contact angle goniometry. *Soft Matter* **15**, 7089–7096 (2019).

40. Group 1 of the Joint Committee for Guides in Metrology (JCGM/WG1). Evaluation of measurement data — Guide to the expression of uncertainty in measurement. Int. Organ. Stand. Geneva ISBN 50, 134. https://doi.org/10.59161/JCGM100-2008E (2008) doi:10.59161/JCGM100-2008E.

41. Guimarães Couto, P. R., Carreteiro, J. & de Oliveir, S. P. Monte Carlo Simulations Applied to Uncertainty in Measurement. in *Theory and Applications of Monte Carlo Simulations* (InTech, 2013). doi:10.5772/53014.

42. Lam, C. W. E. *et al.* Condensate droplet roaming on nanostructured superhydrophobic surfaces. *Nat. Commun.* **16**, 1167 (2025).

43. Mohammad Karim, A., Davis, S. H. & Kavehpour, H. P. Forced versus spontaneous spreading of liquids. *Langmuir* **32**, 10153–10158 (2016).

44. Butt, H. J., Berger, R., Steffen, W., Vollmer, D. & Weber, S. A. L. Adaptive Wetting - Adaptation in Wetting. *Langmuir* **34**, 11292–11304 (2018).

45. Blake, T. D. The physics of moving wetting lines. *J. Colloid Interface Sci.* **299**, 1–13 (2006).

46. Uyama, Y., Inoue, H., Ito, K., Kishida, A. & Ikada, Y. Comparison of Different Methods for Contact Angle Measurement. *J. Colloid Interface Sci.* **141**, 275–279 (1991).

47. The European Parliament and The Council of the European Union. *Regulation (EU) 2024/573 of the European Parliament and of the Council of 7 February 2024 on Fluorinated Greenhouse Gases, Amending Directive (EU) 2019/1937 and Repealing Regulation (EU) No 517/2014*. (2024).

48. McLinden, M. O., Brown, J. S., Brignoli, R., Kazakov, A. F. & Domanski, P. A. Limited options for low-global-warming-potential refrigerants. *Nat. Commun.* **8**, 14476 (2017).

49. Cattelan, G., Diani, A. & Azzolin, M. Condensation heat transfer of R1234ze(E) and R134a inside a brazed plate heat exchanger: Experimental data and model assessment. *Int. J. Refrig.* **143**, 57–67 (2022).

50. Mattiuzzo, N., Berto, A., Azzolin, M. & Del Col, D. Experimental analysis and modelling of R1233zd(E) condensation heat transfer and pressure drop in small diameter channels. *Therm. Sci. Eng. Prog.* **62**, 103586 (2025).

51. Fu, G.-T., Zhang, K. & Fan, L.-W. Advancing and Receding Contact Angles of Water on a Hydrophobic Surface: High-Temperature and High-Pressure Insights. *Langmuir* **41**, 21177–21189 (2025).

52. Urata, C., Masheder, B., Cheng, D. F. & Hozumi, A. How to reduce resistance to movement of alkane liquid drops across tilted surfaces without relying on surface roughening and perfluorination. *Langmuir* **28**, 17681–17689 (2012).

53. Urata, C. *et al.* Why can organic liquids move easily on smooth alkyl-terminated surfaces? *Langmuir* **30**, 4049–4055 (2014).

54. Wassgren, J. & Hozumi, A. Recent Progress on Fluorine-Free Smooth and Textured Surfaces Exhibiting (Super)omniphobicity and Their Future Prospects. *ACS Nano* **19**, 27075–27115 (2025).

55. Schrader, M. E. Wettability of Clean Metal Surfaces. *J. Colloid Interface Sci.* **100**, 372–380 (1984).

56. Enright, R., Miljkovic, N., Alvarado, J. L., Kim, K. & Rose, J. W. Dropwise condensation on micro-and nanostructured surfaces. *Nanoscale Microscale Thermophys. Engineering* **18**, 223–250 (2014).

57. Zisman, W. A. Relation of the Equilibrium Contact Angle to Liquid and Solid Constitution. in *Contact Angle, Wettability, and Adhesion* 1–51 (American Chemical Society, 1964). doi:10.1021/ba-1964-0043.ch001.

58. Eral, H. B., 'T Mannetje, D. J. C. M. & Oh, J. M. Contact angle hysteresis: A review of fundamentals and applications. *Colloid Polym. Sci.* **291**, 247–260 (2013).

59. de Gennes, P. G. Wetting: statics and dynamics. *Rev. Mod. Phys.* **57**, 827–863 (1985).

60. Sharbati, P., Sadaghiani, A. K. & Koşar, A. On the effect of static and dynamic contact angles on humid air condensation heat transfer. *Int. J. Heat Mass Transf.* **219**, 124929 (2024).

61. Ramé, E. The Interpretation of Dynamic Contact Angles Measured by the Wilhelmy Plate Method. *J. Colloid Interface Sci.* **185**, 245–251 (1997).

62. Mohammad Karim, A. & Kavehpour, H. P. Effect of viscous force on dynamic contact angle measurement using Wilhelmy plate method. *Colloids Surf. A Physicochem. Eng. Asp.* **548**, 54–60 (2018).

Funding

This research was supported by the “Centre Giorgio Levi Cases for Energy Economics and Technology” of the University of Padova, under the project “Liquid-like Surfaces for Sustainable and Enhanced Dropwise Condensation of Water Vapor”. Funding was awarded to M.T.

Data Availability

Correspondence and requests for research data should be addressed to Marco Tancon, Marco Azzolin or Stefano Bortolin.